National Oceanography Centre, Southampton

Internal Document No. 12

Analysis of shipboard ADCP data from RRS *Discovery* Cruise D324: RAPID Array Eastern Boundary

C Atkinson

2008

National Oceanography Centre, Southampton
University of Southampton, Waterfront Campus
European Way
Southampton
Hants SO14 3ZH
UK

Author contact details
Tel: +44 (0)23 8059 6488
Email: cpa105@noc.soton.ac.uk

DOCUMENT DATA SHEET

AUTHOR
ATKINSON, C

PUBLICATION DATE 2008

TITLE
Analysis of shipboard ADCP data from RRS Discovery Cruise D324: RAPID Array Eastern Boundary.

REFERENCE
Southampton, UK: National Oceanography Centre, Southampton, 16pp.
(National Oceanography Centre Southampton Internal Document, No. 12)
(Unpublished manuscript)

ABSTRACT

Analysis of underway ADCP data from cruise D324 (RAPID Array Eastern Boundary) revealed three potential biases in the measurements. An investigation of these features is presented here, along with a physical explanation or strategy for removal where appropriate. The first feature is a series of barotropic velocity bands in the along and cross track measurements. These cannot be explained by either heading correction errors or tidal motions, implying a strong eddy field at 26N during the period of observation. The second feature is an along track forward bias caused by bubble interference with the ADCP signal. A strategy for removal is presented using filters applied to raw ADCP data, however future implementation is only recommended with careful selection of suitable filter parameters. The final feature is an S-shaped along-track velocity bias resulting from interaction of ADCP side-lobes with a strong biological scattering horizon while underway. Similar biases have been observed elsewhere in the ocean and a physical explanation is given. A description of ADCP setup, data processing routines and a comparison with geostrophic velocities calculated from CTD dips is also presented.

KEYWORDS
ADCP, bias, side-lobe

ISSUING ORGANISATION
National Oceanography Centre, Southampton
University of Southampton, Waterfront Campus
European Way
Southampton SO14 3ZH
UK

Analysis of Shipboard ADCP Data (Ocean Surveyor 75kHz) from Cruise D324.

Chris Atkinson

1. Introduction

The aim of this document is to make the reader aware of the potential biases that were observed in the ADCP data during cruise D324. This document comprises much of the ADCP section from the D324 cruise report (Eastern Atlantic RAPID mooring recovery) with some additional figures and text for clarity. The potential biases that were observed are discussed in sections 4.1.3, 4.1.4 and 4.1.5, including a physical explanation or strategy for removal where appropriate. The other sections from the original ADCP report have been included for completeness. The approximate cruise track for D324 is shown in figure 1 (Tenerife to the Mid Atlantic Ridge (MAR) to Tenerife along a mostly zonal track).

2. Setup

The 75kHz ADCP is a narrow band phased array with a 30-degree beam angle. Data was logged on a PC, using RDI data acquisition software. The instrument was configured to sample over 120 second intervals, with 60 bins of 16m thicknesses, and a blank beyond transmit of 8 m. Data were averaged into 2 minute averaged files (Short Term Averaging, file extension STA) and 10 minute averaged files (Long Term Averaging, file extension LTA). The former were used for all data processing. The software logs the PC clock time and its offset from GPS time. This offset was applied to the data during processing, before merging with navigation data streams. Gyro heading and GPS Ashtech heading, location and time were fed as NMEA messages into the software, which was configured to use gyro heading for coordinate transformation. During post-processing, gyro heading was corrected to the more accurate but less stable Ashtech heading.

3. Processing

N.B. Routines for this cruise available at: /noc/ooc/rpdmoc/d324

Data were logged on the OS75 PC and transferred by ftp to the UNIX workstation Discovery2ng (cross-mounted with UNIX workstation Sohydro6). Data processing was as follows:

surexec0 — *Performed on Discovery2ng*. Reads data into PSTAR format from RDI data file and edits header information. Writes water track data into the form sur324nn.raw where nn is a user defined code. Scales velocities to cm/s, tracking depth and beam range to metres. Sets bindepth including an offset for depth of transducer and blank beyond transmission. Calculates time in seconds and combines GPS data to correct for PC clock drift.

surexec0b *All further routines performed on Sohydro6*. Extracts data corresponding to one day to create a raw file for this day only, using raw files from *surexec0*.

surexec1 Edit out bad data and replace with absent data (-999). Data removed where beam 1 status (status1) is flagged as one (bad data) and 2+bmbad parameter is > 25% (percentage of pings where 2 or more beams were bad therefore no velocity computed). Time stamp moved to end of each ensemble.

surexec2 Merge data with Ashtech-Gyro heading correction (from master Ashtech file ash324i1.int) to correct heading and find true North and East components of current velocity.

surexec3 Calibrate velocities by scaling factor A and by ADCP misalignment angle phi.

surexec4 Calculate absolute current velocities by merging with navigation data and removing ship speed over ground from calibrated velocities. Up to day 299, navigation data from the Trimble 4000 were used. After failure of this instrument on day 300, *surexec4* was edited to use Ashtech GPS12 data instead.

Finally, *surapend.exec* was used to append all final absolute velocity files into one master file sur324apend.abs. sur324apend2.abs and sur324_apendsurf.abs master files were also created containing absolute velocity in the format speed/heading and surface bin data only for comparison to the Chernikeeff. *plot_os75_d324.m* was used to load and plot OS75 data averaged over 3 hours (sur324apend2.3hr), to remove velocities outside limits of +/- 100 cms^{-1} (when the GPS did not receive a differential correction term), and to interpolate over longitude to create longitudinally averaged velocities. *CTD_OS75.m* was used to load, plot and compare OS75 velocities to geostrophic velocities calculated from CTD dips using the PEXECs pgridp and pgeost. OS75 velocities were rotated into components parallel and perpendicular to the plane of a CTD section, edited for velocities outside limits of +/-100 cms^{-1}, interpolated longitudinally and averaged over each depth bin.

4. Analysis

4.1 OS75 Data

Figure 2 shows OS75 velocities (top) and backscatter intensities for each of the four ADCP beams (bottom) averaged longitudinally (from 20°W to 50°W) for the period heading to the MAR (days 289-300) and returning from the MAR (days 300-308). Velocities are averaged to a bin depth of 600 metres. Below this depth, the range of the ADCP is approached and the removal of bad data by the routine *surexec1* (see section 3) leads to frequent gaps in the dataset. Averaging across these would lead to biases in velocity and intensity at greater depths and these are therefore not shown.

4.1.1 Meridional Ocean Velocities.

For the meridional velocity component (see figure 2 top), a southward shear of approximately 1 cms^{-1} is observed in the upper 60m of the water column. During transit to the MAR, northerly currents are observed between 60-100m depths up to a maximum of 0.5 cms^{-1} at 80m. Below 100m, weak currents up to a maximum of 0.5

cms^{-1} are observed, gradually changing from a southerly to northerly flow as depth increases with a depth of zero motion at approximately 400m. During transit returning from the MAR, the northward velocity profile changed broadly barotropically such that southward flow above 400m increased by 0.5 to 1 cms^{-1}. This may be a result of aliasing barotropic variability over time. Below 450m, a southward shear of 1 cms^{-1} is seen to develop.

4.1.2 Zonal Ocean Velocities.

For the zonal velocity component (see figure 2 top), several erroneous features are noted. Of particular note is a large increase in ocean velocity between 350 and 480 metre depths for transit both to and from the MAR, and a sizeable peak in ocean velocity (up to 7 cms^{-1}) in the upper 100 metres of the water column for return transit from the MAR. These are discussed in sections *4.1.4* and *4.1.5*.

4.1.3 Ocean Velocity Banding

Variability of the zonal and meridional components of velocity over time is mostly barotropic, with fluctuations typically up to ±10-15 cms^{-1} observed between diurnal and daily periods (figure 3 top and middle respectively). A first look would suggest meridional velocity (essentially cross-track velocity for an east-west cruise) shows more defined banding than zonal velocity (along-track). This potentially is a concern as vertical velocity banding, particularly where cross-track banding appears of greater magnitude, can be linked to a heading error (correction of gyro heading to GPS heading). Analysis of the heading correction suggests it improves the data, with large spikes in heading correction attributable to periods of ship manoeuvring (where a 'sticky' gyro means large errors) and small oscillations in heading correction related to oscillations in the gyro while underway. Also, standard deviation of cross track and along track velocities at various depths are comparable, suggesting cross track velocities are not in fact more clearly defined as would be expected for a heading error. Although other errors may exist in the data, at this stage there is no reason to doubt the data.

The diurnal like period of the banding may suggest a strong tidal signal within the data. Comparison of ADCP velocities to velocities predicted from a tidal model (using the Matlab Tidal Model Driver which accessed harmonic tidal constituents output from the OSU 0.25 x 0.25 Deg. global assimilation model) does not match in either phase or magnitude (figure 4). The tidal model is thought to be relatively reliable at 26N as it's harmonic constituents match moored ADCP data reasonably well. It should be noted that the phase of the tidal signal measured by the ship will be somewhat distorted where the ship is steaming between mornings, however a large discrepancy in magnitude is still observed. Although a tidal effect undoubtedly contributes to the data, other factors, such as a strong eddy field, could in part be responsible for the observations.

4.1.4 Bubble Bias

The velocity peak in the upper 100 metres of the water column in figure 2 (top) is a result of bubble interference with the ADCP signal that produces a forward bias in the along track measurements. Figure 3 (top) shows this is mostly attributable to a period

of unusually high surface ocean velocities (up to 50 cms^{-1}) recorded between days 303 to 305. This coincided with a swing to strong easterly winds (up to 8 ms^{-1}), a decrease in the ships eastward velocity and increased ship pitch, leading to more bubbles entrained below the ships hull.

With assistance from Dr. Julia Hummon (University of Hawaii), this bubble bias was further investigated. A closer analysis of the singleping xxx.enx files for the period of bubble bias revealed two distinct types of biased profile, typical of bubble interference. These are short, truncated profiles (<200m) biased in the direction of ship motion and longer profiles showing a strong surface shear in the direction of ship motion (figures 5 and 6, examples 1a and 1b are short truncated profiles, example 2a is a longer profile with surface shear). When averaged to form xxx.sta files, a strong surface bias in the direction of ship motion is seen. Currently, no procedure is in place to deal with these bad .enx files and as such, the procedure for removing bad data would be to remove by hand the top x bins of data from the xxx.sta files where a strong bias is seen. However, the depth of strong shear is variable over the top 6 bins of the data, and this procedure risks keeping bad data, removing good data or removing a real shear from the data. Applying algorithms to the raw xxx.enx data can more reliably reduce this bias. Using a single day of biased data, algorithms were applied that removed short profiles and removed shear outliers before averaging. Data showing a degraded % good measurement near the surface were then removed. The effect of this latter processing is to successfully remove much of the bubble bias from the profiles, see figure 7.

The ADCP Command File, D324wat.txt, configures the ADCP to run in Broadband mode. However, the Software Initialisation File D324wat.ini, indicated the system was setup in Narrowband mode. The system was confirmed to be running in Broadband mode. Most of the bubble bias observed was of the second type above (long profiles, strong surface shear) and this may characterise Broadband bubble signature. However, further experiments would be required to confirm this (comparing Narrow and Broadband with interleaved with periods with and without bubble activity).

Recommendation: where a strong bubble bias is seen, processing of the raw .enx data using algorithms (as described above) with filters chosen for the particular data set should help remove bad data, while keeping as much good data as possible. Automated application of these algorithms to future data would not be recommended without further study to choose suitable filter parameters.

4.1.5 High Intensity Backscatter 'Steaming' Bias

The velocity peak between 350 and 480 metres appears to be a 'steaming bias' i.e. a bias created along track in the direction of ship motion. This cannot be attributable to GPS ship speed error as this would lead to a bulk offset of the profile throughout the water column. Figure 3 (top) shows this feature becomes readily apparent from day 293 onwards, changing sign as the ship returned from the MAR after day 300. The meridional component of velocity was measured across ship track for the majority of this 24N cruise and does not show any anomalous features. Between 400 to 500 metre depths, a layer of high backscatter intensity was continuously observed between Tenerife and the MAR (figure 3, bottom). This deepened by approximately 50 metres

from the Eastern to Central Atlantic, comparable to the Eastern Atlantic thermocline. In figure 2 (bottom), this feature is seen more clearly for all of the ADCP beams. Figure 3 (bottom) also shows this high intensity layer migrates diurnally, with a rise to shallow depths of several hundred metres beginning at sunset and return to increased depth beginning shortly before sunrise. Coincident with this is a deepening of the high intensity shallow layer of several tens of metres just after sunset, and a shallowing just before sunrise. This is characteristic of zooplankton diurnal migration, either to feed or to avoid predation. The diurnal reduction of the range of the ADCP (figure 3 top) is also characteristic of the increase of this biological particulate matter in shallow depths during the night time.

This along track velocity bias caused by high scattering layers (in this case zooplankton) has been observed elsewhere in the oceans. Physically it is explained by the side lobes adjacent to the main ADCP beam (transmitted at ~30°) interacting with a high scattering layer (see figure 8, courtesy of Dr. Julia Hummon, University of Hawaii). A side lobe beam transmitted at a shallow angle (< 30°) has a smaller travel time to and from a given depth, Z2, than a beam emitted at 30°. The return from this beam is therefore attributed to a shallower depth, Z1, by the ADCP software. Because the beam is emitted at a shallow angle (relative to vertical), the Doppler shift of the beam during emission **while underway** is reduced, the return signal is of lower frequency than would be expected if the beam were emitted at 30°, and the ocean velocity measured relative to the ship is biased towards zero. When adding ocean velocity (relative to the ship) to ship velocity (relative to earth) to calculate absolute ocean velocities, a bias therefore remains in the direction of ship motion at depths shallower than the scattering layer. This effect is reversed for side lobe beams emitted at a steeper angle (relative to vertical) leading to a bias in absolute ocean velocities opposite to ship motion at depths below the scattering layer. Although side lobes contain less energy than the main beam at 30°, the presence of a strong scattering layer mean their effects become noticeable and in this case dominant. This effect is not noted in across track velocities because there is much less Doppler shift during beam emission perpendicular to the direction of ship motion.

The result of this 'high backscatter layer' is an 'S' shaped bias in ocean velocity measurements, with a crossing point centred on the high backscatter layer itself. The 'S' can extend to a range of several bins above and below the centre of the high backscatter layer. This bias is present in the ADCP velocities shown in figure 2 (top) from approximately 350 metre depths to the range of the instrument. However, because of the limited range of the ADCP, the full 'S' shape of the bias cannot be discerned. When ship velocity reduces, this bias should also reduce and eventually disappear. Figure 9 shows ship speed measured by the GPS (top), hourly velocity profiles measured by the ADCP (middle) and three-hourly backscatter intensity (bottom) for the period surrounding CTD casts 8 and 9. Although the high scatter layer is present throughout, the velocity bias diminishes during periods of reduced ship speed for CTD operations. This contrasts with figure 10, showing ADCP measurements during the transit from Falmouth to Tenerife. Although an error with the GPS led to a reduced number of available ocean velocity profiles, it is still evident that during periods of steaming, there is no ADCP velocity bias at depth because no strong backscattering layer is present. Further plots (not shown) show that this deep scattering layer is present shortly after leaving Tenerife (day 288). The bias is not as evident in figure 3 (top) during this period because the south westerly heading of the

ship prior to day 292 means some component of the zonal velocity is measured across track which reduces the impact of this along track bias. No method for removing this bias attributable to a deep scattering layer is apparent. Because some of the zooplankton layer remains in situ (at 470 metres) both night and day (i.e. does not migrate diurnally, see figure 3 bottom), the velocity bias is present throughout the whole ADCP dataset and therefore little good data for this depth range are available. The persistence of such signals in single-ping .ENX data would be worth investigating to see if any data could be salvaged at depth where a strong scattering layer occurs.

4.2 OS75-Geostrophy Comparison

Comparison of ADCP data to geostrophic velocities calculated between CTD stations 5-10 in the upper water column are shown in figure 11. Data shown was collected during transit to the MAR and for geostrophic purposes assumes a depth of no motion at 3200 metres. The CTD data used was not calibrated to samples collected on D324 however the CTD was relatively well calibrated at the start of the trip. The effect of erroneous E-W ADCP velocity measurements (discussed above) is small due to predominant analysis of the N-S component of ADCP measurements. Of particular note are the velocity profiles averaged between station pair 7-8 (between 23-41W and covering the widest area). Geostrophic velocity decreases steadily from -1.5 cms^{-1} at the surface to 0 cms^{-1} at 1000m, while the ADCP velocity shows broadly similar structure (except above 50m depths where inertial effects dominate) but offset such that velocity approaches +1.5 cms^{-1} at 600m. Adjustment of geostrophic velocity to match this absolute velocity would lead to anomalously large ocean transports at depth. Velocities between stations 6 and 7 again show broadly similar profiles but are offset. Little agreement is seen between absolute ADCP velocity and geostrophic velocity for station pairs 5-6 and 8-10 (the latter over the MAR).

5. Conclusion

The setup, processing and results from the underway ADCP during cruise D324 have been described. Of particular note are three potential biases observed in the data. The first of these is a series of vertical velocity bands (10-15 cms^{-1} magnitude) observed in both the along track and cross track measurements. A heading error is ruled out as the source of this signal, suggesting the banding observed is real. Comparison with a tidal model suggests velocity bands are not of tidal origin, implying a strong eddy field. The second bias is an along track forward bias caused by bubble interference with the ADCP signal. It is shown that this bubble bias produces two distinct velocity profile types, which can be removed from the measurements by applying filters to the raw, single-ping .ENX files. Algorithms are applied that remove short profiles and shear outliers before averaging to .STA files. Data showing a degraded % good measurement near the surface are then also removed. Application of such algorithms is recommended in the future where appropriate, however care should be taken to choose suitable filter parameters for a particular dataset. The final bias is an S-shaped velocity structure in the along track data that appears due to interaction of the ADCP side lobes with a strong scattering horizon. This bias relies on differences in Doppler shift between the side lobe and main beams during emission and as such is only observed while underway. The absence of the bias during periods when the ship was stationary or when no scattering layer was observed is demonstrated. Diurnal

migration of the strong scattering layer (seen in ADCP backscatter intensity measurements) suggests it is a biological horizon. ADCP data are contaminated by this bias for the duration of D324. Similar velocity biases have been observed elsewhere in the ocean.

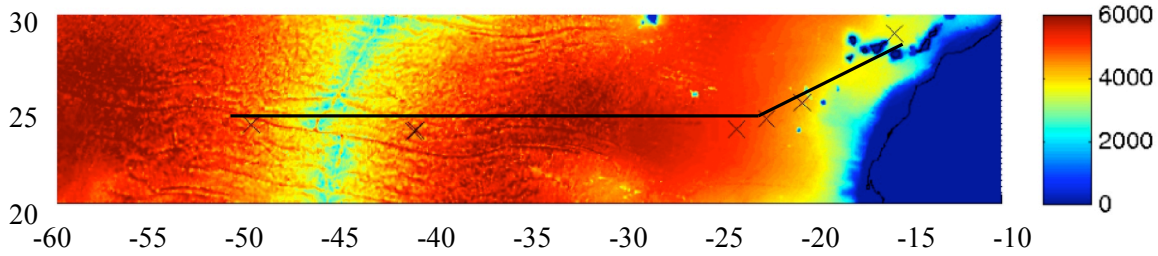

Figure 1, D324 Cruise Track on bathymetric map (longitude vs. latitude, depth in metres).

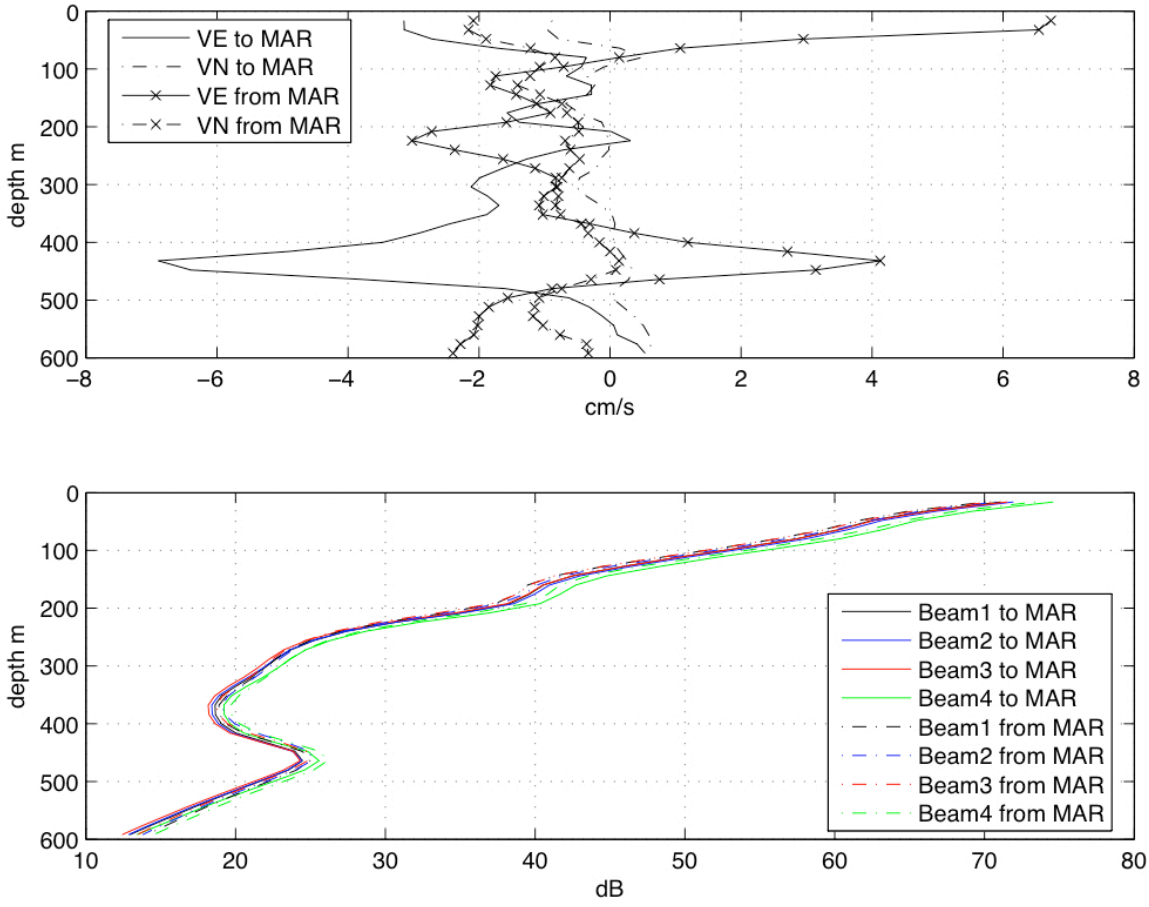

Figure 2. Meridional (VN) and zonal velocity (VE) components (top) and beam intensity (bottom) measured by the ADCP during transit to and from the MAR during D324. Bins are averaged longitudinally between 20 and 50 W.

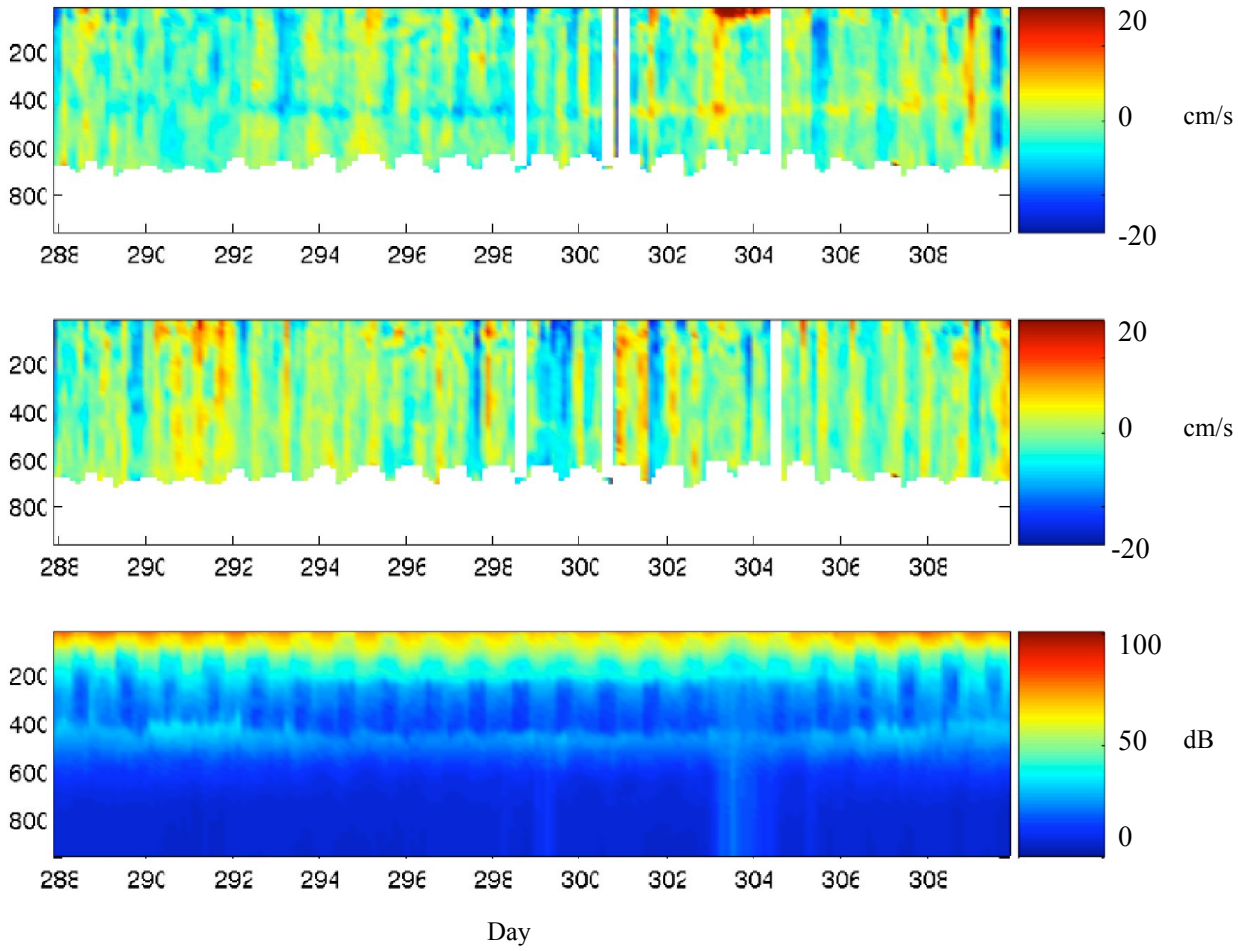

Figure 3. Zonal ocean velocity (top), meridional ocean velocity (middle) and beam 1 intensity (bottom) against depth (m) measured by the ADCP during transit to and from the MAR during D324.

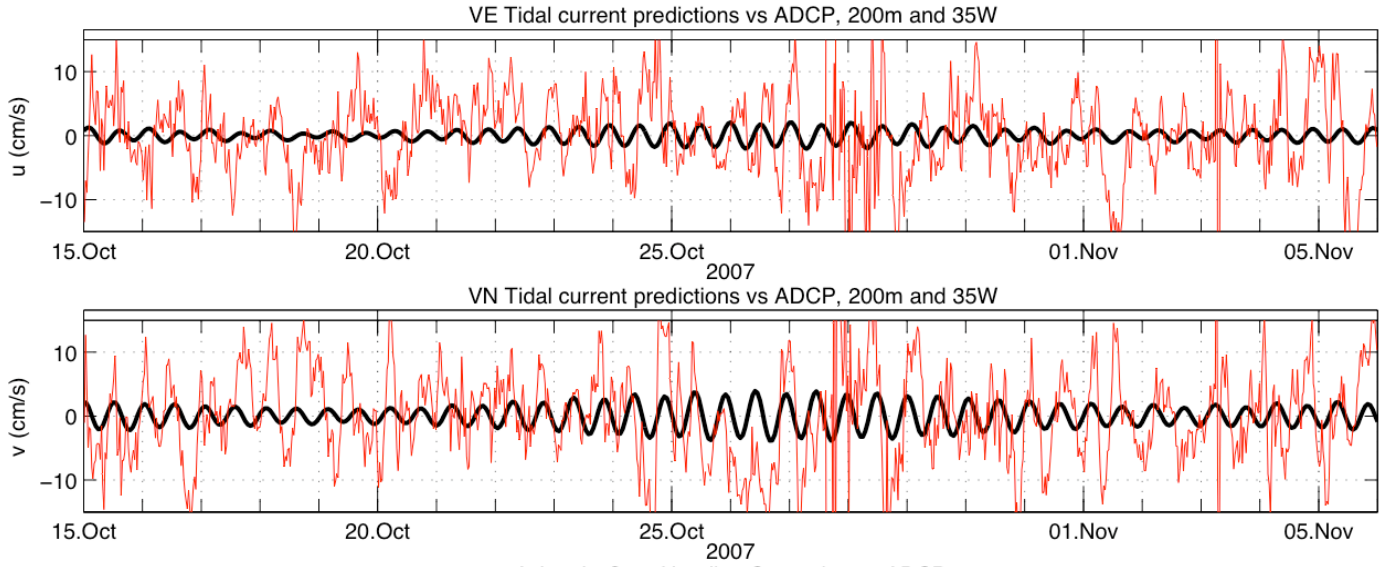

Figure 4. ADCP (red lines) zonal (top) and meridional (bottom) velocities during cruise D324 and tidal velocities (black lines) predicted from a tidal model. Velocities are shown at 200m depth. Tidal velocities are calculated using harmonic constituents at 26N, 35W (note, tidal harmonics are relatively longitudinally invariant at this latitude).

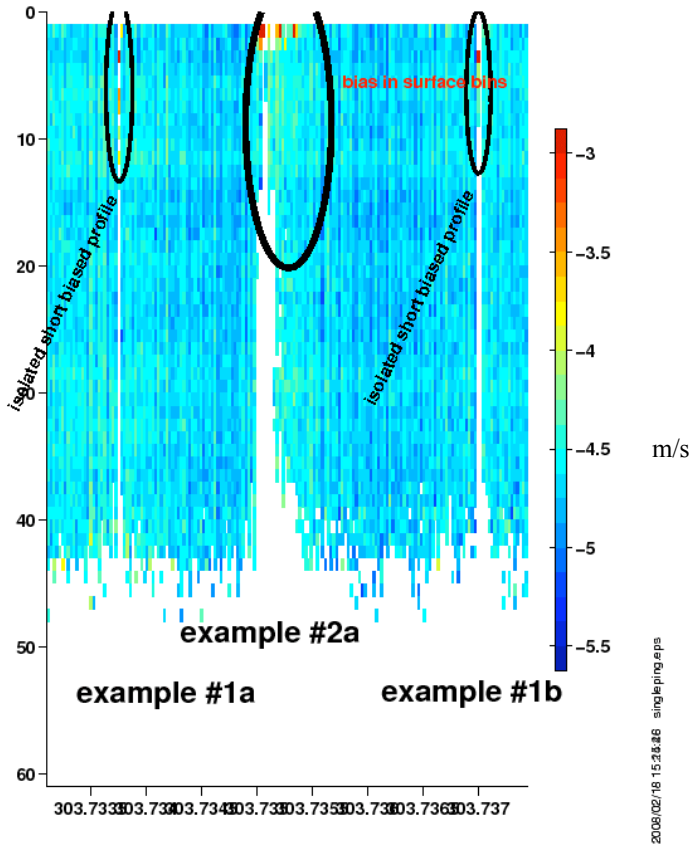

Figure 5. Plot showing single-ping (.ENX) along track velocities versus bin number for part of day 303. Two types of bubble related bias are highlighted. Courtesy of Julia Hummon, University of Hawaii.

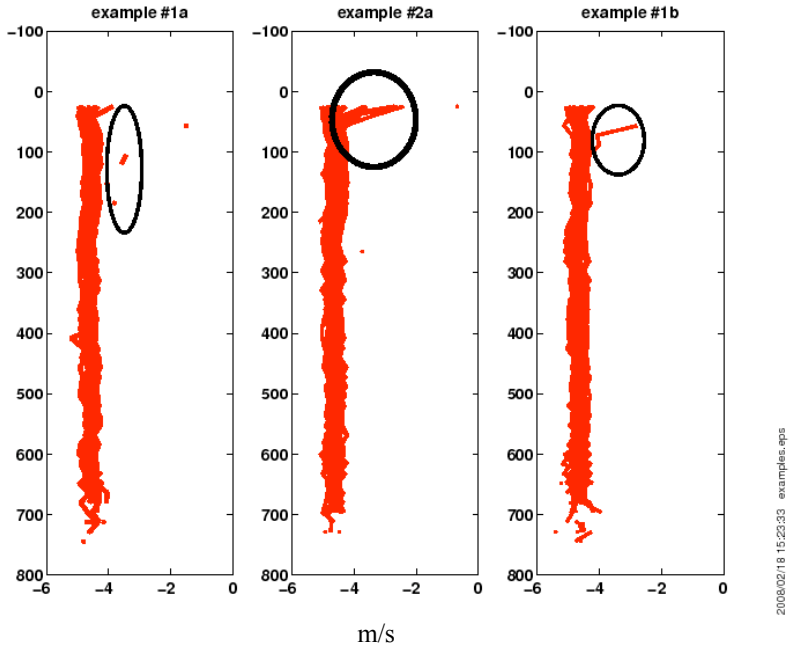

Figure 6. Along track velocity profiles of two types of bubble bias highlighted in figure 4. Courtesy of Julia Hummon, University of Hawaii.

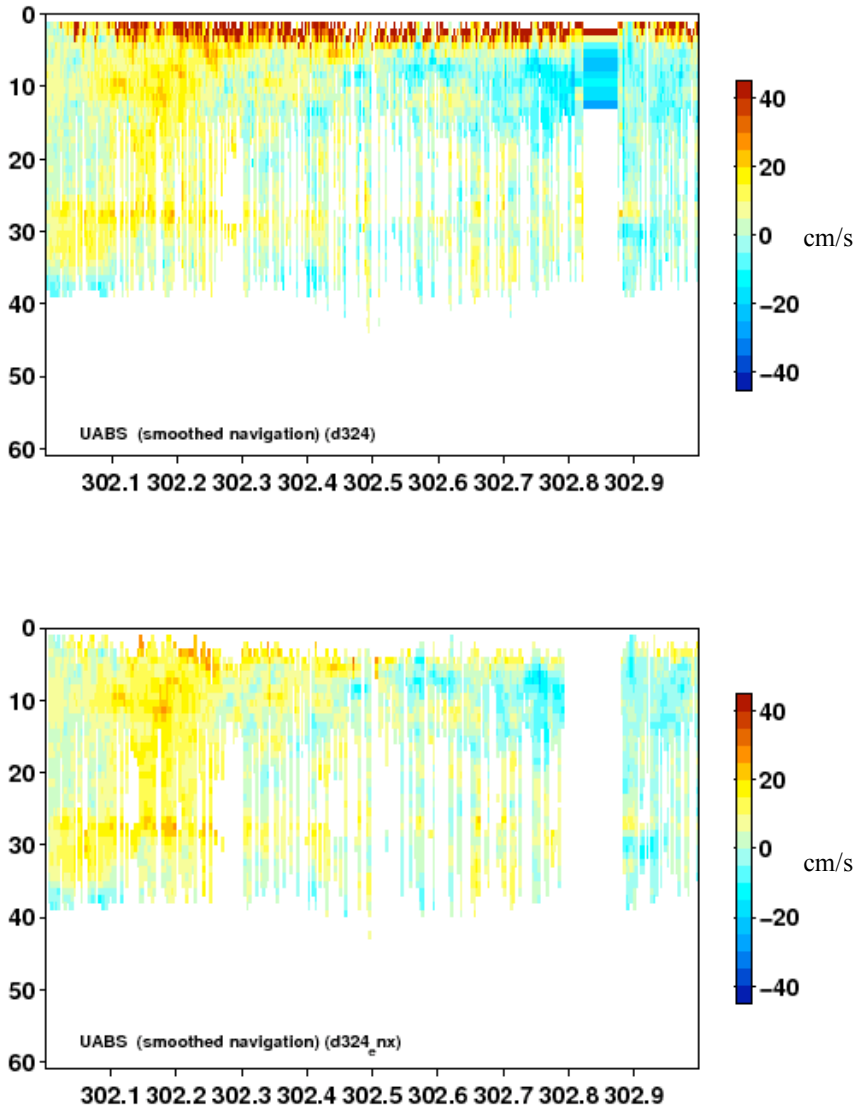

Figure 7. Plots of zonal velocity versus bin number for day 303. Top shows .STA data without .ENX editing routines. Bottom shows .STA data formed using edited .ENX files. Courtesy of Julia Hummon, University of Hawaii.

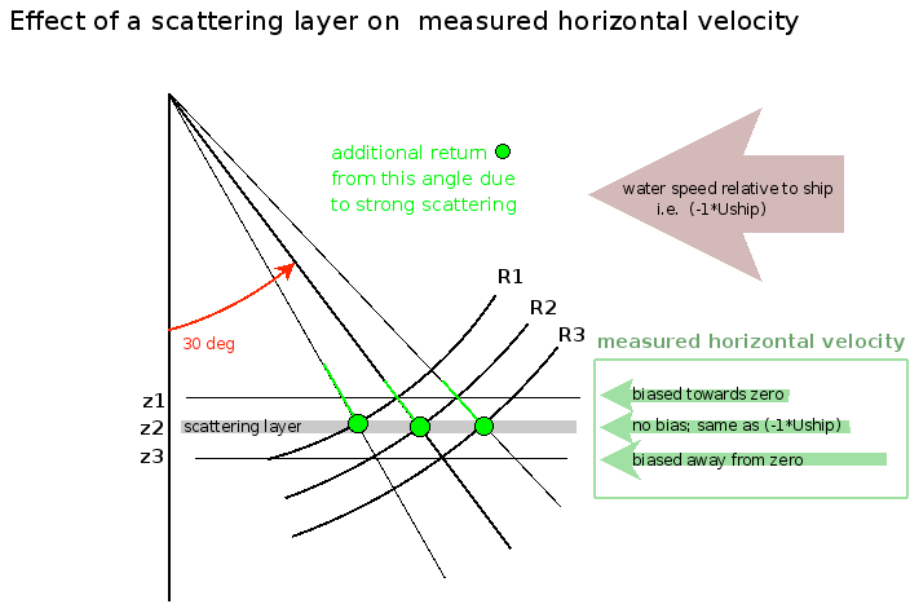

Figure 8. Schematic diagram demonstrating the effects of a strong scattering layer on an ADCP beam and measured velocities (courtesy Julia Hummon, University of Hawaii), see text for explanation.

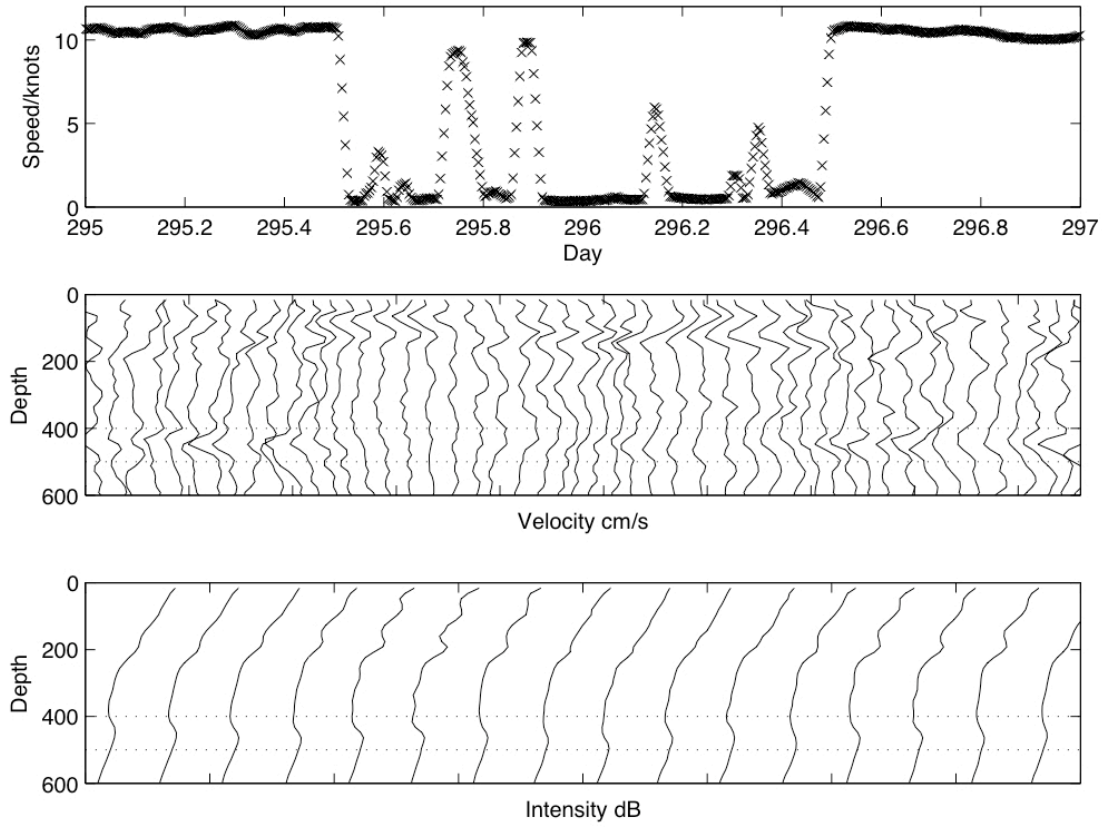

Figure 9. Ship speed (top), hourly velocity profiles (middle), and three hourly ADCP beam 1 intensity profiles (bottom) for from day 295 to 297. Depths of interest are highlighted by stippled lines. One velocity axis tick corresponds to 50 cms^{-1}, one intensity axis tick corresponds to 100 dB.

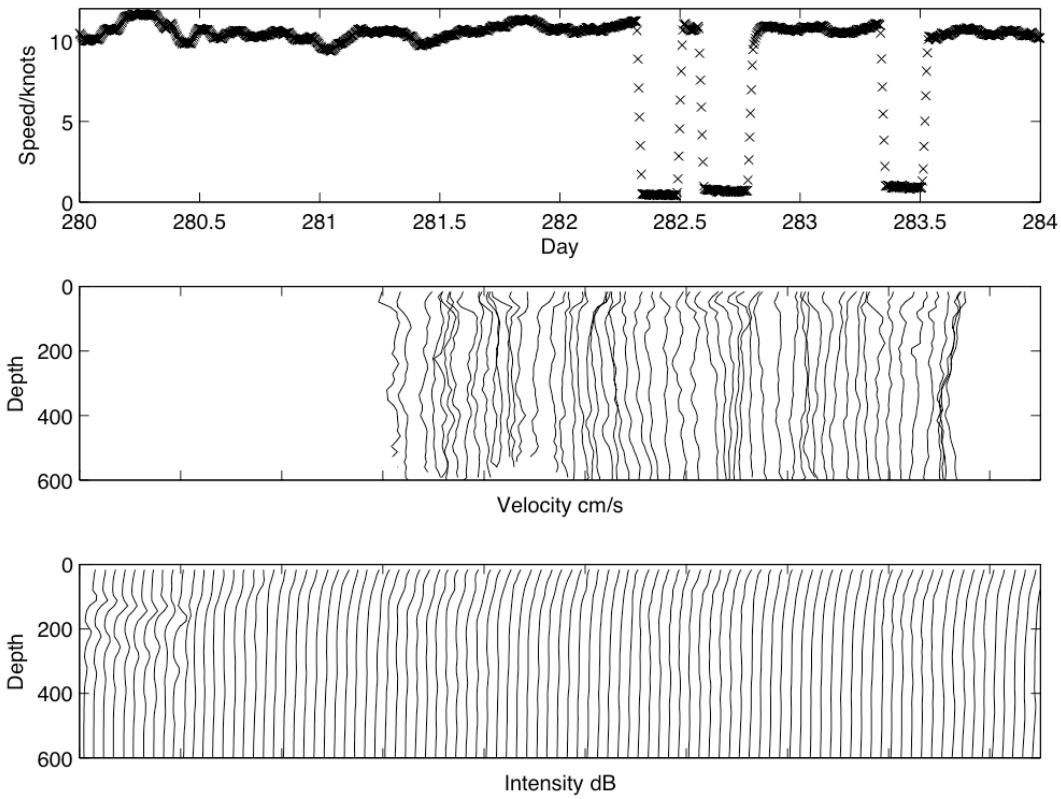

Figure 10. As for figure 8, ADCP beam 1 intensities (bottom) are shown hourly. Velocity data is absent for much of the transit due to a GPS error.

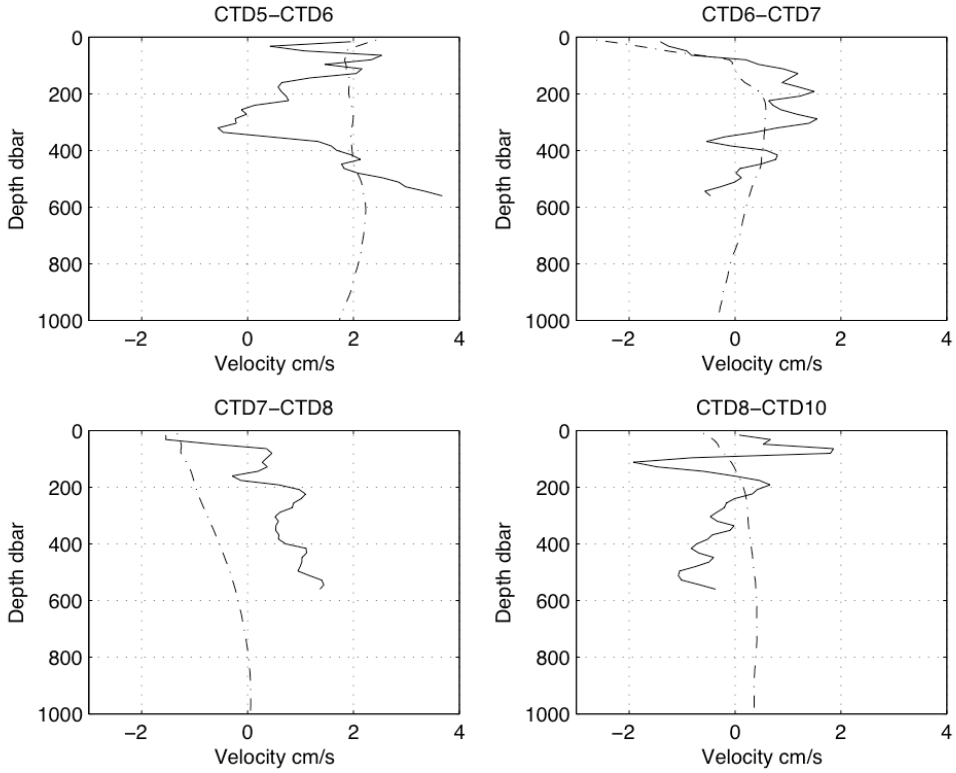

Figure 11. Geostrophic velocities (stippled line) and ADCP velocities (solid lines) averaged between CTD station pairs.

DOCUMENT DATA SHEET

AUTHOR
ATKINSON, C

PUBLICATION DATE 2008

TITLE
Analysis of shipboard ADCP data from RRS Discovery Cruise D324: RAPID Array Eastern Boundary.

REFERENCE
Southampton, UK: National Oceanography Centre, Southampton, 16pp.
(National Oceanography Centre Southampton Internal Document, No. 12)
(Unpublished manuscript)

ABSTRACT

Analysis of underway ADCP data from cruise D324 (RAPID Array Eastern Boundary) revealed three potential biases in the measurements. An investigation of these features is presented here, along with a physical explanation or strategy for removal where appropriate. The first feature is a series of barotropic velocity bands in the along and cross track measurements. These cannot be explained by either heading correction errors or tidal motions, implying a strong eddy field at 26N during the period of observation. The second feature is an along track forward bias caused by bubble interference with the ADCP signal. A strategy for removal is presented using filters applied to raw ADCP data, however future implementation is only recommended with careful selection of suitable filter parameters. The final feature is an S-shaped along-track velocity bias resulting from interaction of ADCP side-lobes with a strong biological scattering horizon while underway. Similar biases have been observed elsewhere in the ocean and a physical explanation is given. A description of ADCP setup, data processing routines and a comparison with geostrophic velocities calculated from CTD dips is also presented.

KEYWORDS
ADCP, bias, side-lobe

ISSUING ORGANISATION
National Oceanography Centre, Southampton
University of Southampton, Waterfront Campus
European Way
Southampton SO14 3ZH
UK

Analysis of Shipboard ADCP Data (Ocean Surveyor 75kHz) from Cruise D324.

Chris Atkinson

1. Introduction

The aim of this document is to make the reader aware of the potential biases that were observed in the ADCP data during cruise D324. This document comprises much of the ADCP section from the D324 cruise report (Eastern Atlantic RAPID mooring recovery) with some additional figures and text for clarity. The potential biases that were observed are discussed in sections 4.1.3, 4.1.4 and 4.1.5, including a physical explanation or strategy for removal where appropriate. The other sections from the original ADCP report have been included for completeness. The approximate cruise track for D324 is shown in figure 1 (Tenerife to the Mid Atlantic Ridge (MAR) to Tenerife along a mostly zonal track).

2. Setup

The 75kHz ADCP is a narrow band phased array with a 30-degree beam angle. Data was logged on a PC, using RDI data acquisition software. The instrument was configured to sample over 120 second intervals, with 60 bins of 16m thicknesses, and a blank beyond transmit of 8 m. Data were averaged into 2 minute averaged files (Short Term Averaging, file extension STA) and 10 minute averaged files (Long Term Averaging, file extension LTA). The former were used for all data processing. The software logs the PC clock time and its offset from GPS time. This offset was applied to the data during processing, before merging with navigation data streams. Gyro heading and GPS Ashtech heading, location and time were fed as NMEA messages into the software, which was configured to use gyro heading for coordinate transformation. During post-processing, gyro heading was corrected to the more accurate but less stable Ashtech heading.

3. Processing

N.B. Routines for this cruise available at: /noc/ooc/rpdmoc/d324

Data were logged on the OS75 PC and transferred by ftp to the UNIX workstation Discovery2ng (cross-mounted with UNIX workstation Sohydro6). Data processing was as follows:

surexec0 — *Performed on Discovery2ng*. Reads data into PSTAR format from RDI data file and edits header information. Writes water track data into the form sur324nn.raw where nn is a user defined code. Scales velocities to cm/s, tracking depth and beam range to metres. Sets bindepth including an offset for depth of transducer and blank beyond transmission. Calculates time in seconds and combines GPS data to correct for PC clock drift.

surexec0b *All further routines performed on Sohydro6*. Extracts data corresponding to one day to create a raw file for this day only, using raw files from *surexec0*.

surexec1 Edit out bad data and replace with absent data (-999). Data removed where beam 1 status (status1) is flagged as one (bad data) and 2+bmbad parameter is > 25% (percentage of pings where 2 or more beams were bad therefore no velocity computed). Time stamp moved to end of each ensemble.

surexec2 Merge data with Ashtech-Gyro heading correction (from master Ashtech file ash324i1.int) to correct heading and find true North and East components of current velocity.

surexec3 Calibrate velocities by scaling factor A and by ADCP misalignment angle phi.

surexec4 Calculate absolute current velocities by merging with navigation data and removing ship speed over ground from calibrated velocities. Up to day 299, navigation data from the Trimble 4000 were used. After failure of this instrument on day 300, *surexec4* was edited to use Ashtech GPS12 data instead.

Finally, *surapend.exec* was used to append all final absolute velocity files into one master file sur324apend.abs. sur324apend2.abs and sur324_apendsurf.abs master files were also created containing absolute velocity in the format speed/heading and surface bin data only for comparison to the Chernikeeff. *plot_os75_d324.m* was used to load and plot OS75 data averaged over 3 hours (sur324apend2.3hr), to remove velocities outside limits of +/- 100 cms^{-1} (when the GPS did not receive a differential correction term), and to interpolate over longitude to create longitudinally averaged velocities. *CTD_OS75.m* was used to load, plot and compare OS75 velocities to geostrophic velocities calculated from CTD dips using the PEXECs pgridp and pgeost. OS75 velocities were rotated into components parallel and perpendicular to the plane of a CTD section, edited for velocities outside limits of +/-100 cms^{-1}, interpolated longitudinally and averaged over each depth bin.

4. Analysis

4.1 OS75 Data

Figure 2 shows OS75 velocities (top) and backscatter intensities for each of the four ADCP beams (bottom) averaged longitudinally (from 20°W to 50°W) for the period heading to the MAR (days 289-300) and returning from the MAR (days 300-308). Velocities are averaged to a bin depth of 600 metres. Below this depth, the range of the ADCP is approached and the removal of bad data by the routine *surexec1* (see section 3) leads to frequent gaps in the dataset. Averaging across these would lead to biases in velocity and intensity at greater depths and these are therefore not shown.

4.1.1 Meridional Ocean Velocities.

For the meridional velocity component (see figure 2 top), a southward shear of approximately 1 cms^{-1} is observed in the upper 60m of the water column. During transit to the MAR, northerly currents are observed between 60-100m depths up to a maximum of 0.5 cms^{-1} at 80m. Below 100m, weak currents up to a maximum of 0.5

cms^{-1} are observed, gradually changing from a southerly to northerly flow as depth increases with a depth of zero motion at approximately 400m. During transit returning from the MAR, the northward velocity profile changed broadly barotropically such that southward flow above 400m increased by 0.5 to 1 cms^{-1}. This may be a result of aliasing barotropic variability over time. Below 450m, a southward shear of 1 cms^{-1} is seen to develop.

4.1.2 Zonal Ocean Velocities.

For the zonal velocity component (see figure 2 top), several erroneous features are noted. Of particular note is a large increase in ocean velocity between 350 and 480 metre depths for transit both to and from the MAR, and a sizeable peak in ocean velocity (up to 7 cms^{-1}) in the upper 100 metres of the water column for return transit from the MAR. These are discussed in sections *4.1.4* and *4.1.5*.

4.1.3 Ocean Velocity Banding

Variability of the zonal and meridional components of velocity over time is mostly barotropic, with fluctuations typically up to ±10-15 cms^{-1} observed between diurnal and daily periods (figure 3 top and middle respectively). A first look would suggest meridional velocity (essentially cross-track velocity for an east-west cruise) shows more defined banding than zonal velocity (along-track). This potentially is a concern as vertical velocity banding, particularly where cross-track banding appears of greater magnitude, can be linked to a heading error (correction of gyro heading to GPS heading). Analysis of the heading correction suggests it improves the data, with large spikes in heading correction attributable to periods of ship manoeuvring (where a 'sticky' gyro means large errors) and small oscillations in heading correction related to oscillations in the gyro while underway. Also, standard deviation of cross track and along track velocities at various depths are comparable, suggesting cross track velocities are not in fact more clearly defined as would be expected for a heading error. Although other errors may exist in the data, at this stage there is no reason to doubt the data.

The diurnal like period of the banding may suggest a strong tidal signal within the data. Comparison of ADCP velocities to velocities predicted from a tidal model (using the Matlab Tidal Model Driver which accessed harmonic tidal constituents output from the OSU 0.25 x 0.25 Deg. global assimilation model) does not match in either phase or magnitude (figure 4). The tidal model is thought to be relatively reliable at 26N as it's harmonic constituents match moored ADCP data reasonably well. It should be noted that the phase of the tidal signal measured by the ship will be somewhat distorted where the ship is steaming between mornings, however a large discrepancy in magnitude is still observed. Although a tidal effect undoubtedly contributes to the data, other factors, such as a strong eddy field, could in part be responsible for the observations.

4.1.4 Bubble Bias

The velocity peak in the upper 100 metres of the water column in figure 2 (top) is a result of bubble interference with the ADCP signal that produces a forward bias in the along track measurements. Figure 3 (top) shows this is mostly attributable to a period

of unusually high surface ocean velocities (up to 50 cms^{-1}) recorded between days 303 to 305. This coincided with a swing to strong easterly winds (up to 8 ms^{-1}), a decrease in the ships eastward velocity and increased ship pitch, leading to more bubbles entrained below the ships hull.

With assistance from Dr. Julia Hummon (University of Hawaii), this bubble bias was further investigated. A closer analysis of the singleping xxx.enx files for the period of bubble bias revealed two distinct types of biased profile, typical of bubble interference. These are short, truncated profiles (<200m) biased in the direction of ship motion and longer profiles showing a strong surface shear in the direction of ship motion (figures 5 and 6, examples 1a and 1b are short truncated profiles, example 2a is a longer profile with surface shear). When averaged to form xxx.sta files, a strong surface bias in the direction of ship motion is seen. Currently, no procedure is in place to deal with these bad .enx files and as such, the procedure for removing bad data would be to remove by hand the top x bins of data from the xxx.sta files where a strong bias is seen. However, the depth of strong shear is variable over the top 6 bins of the data, and this procedure risks keeping bad data, removing good data or removing a real shear from the data. Applying algorithms to the raw xxx.enx data can more reliably reduce this bias. Using a single day of biased data, algorithms were applied that removed short profiles and removed shear outliers before averaging. Data showing a degraded % good measurement near the surface were then removed. The effect of this latter processing is to successfully remove much of the bubble bias from the profiles, see figure 7.

The ADCP Command File, D324wat.txt, configures the ADCP to run in Broadband mode. However, the Software Initialisation File D324wat.ini, indicated the system was setup in Narrowband mode. The system was confirmed to be running in Broadband mode. Most of the bubble bias observed was of the second type above (long profiles, strong surface shear) and this may characterise Broadband bubble signature. However, further experiments would be required to confirm this (comparing Narrow and Broadband with interleaved with periods with and without bubble activity).

Recommendation: where a strong bubble bias is seen, processing of the raw .enx data using algorithms (as described above) with filters chosen for the particular data set should help remove bad data, while keeping as much good data as possible. Automated application of these algorithms to future data would not be recommended without further study to choose suitable filter parameters.

4.1.5 High Intensity Backscatter 'Steaming' Bias

The velocity peak between 350 and 480 metres appears to be a 'steaming bias' i.e. a bias created along track in the direction of ship motion. This cannot be attributable to GPS ship speed error as this would lead to a bulk offset of the profile throughout the water column. Figure 3 (top) shows this feature becomes readily apparent from day 293 onwards, changing sign as the ship returned from the MAR after day 300. The meridional component of velocity was measured across ship track for the majority of this 24N cruise and does not show any anomalous features. Between 400 to 500 metre depths, a layer of high backscatter intensity was continuously observed between Tenerife and the MAR (figure 3, bottom). This deepened by approximately 50 metres

from the Eastern to Central Atlantic, comparable to the Eastern Atlantic thermocline. In figure 2 (bottom), this feature is seen more clearly for all of the ADCP beams. Figure 3 (bottom) also shows this high intensity layer migrates diurnally, with a rise to shallow depths of several hundred metres beginning at sunset and return to increased depth beginning shortly before sunrise. Coincident with this is a deepening of the high intensity shallow layer of several tens of metres just after sunset, and a shallowing just before sunrise. This is characteristic of zooplankton diurnal migration, either to feed or to avoid predation. The diurnal reduction of the range of the ADCP (figure 3 top) is also characteristic of the increase of this biological particulate matter in shallow depths during the night time.

This along track velocity bias caused by high scattering layers (in this case zooplankton) has been observed elsewhere in the oceans. Physically it is explained by the side lobes adjacent to the main ADCP beam (transmitted at ~30°) interacting with a high scattering layer (see figure 8, courtesy of Dr. Julia Hummon, University of Hawaii). A side lobe beam transmitted at a shallow angle (< 30°) has a smaller travel time to and from a given depth, Z2, than a beam emitted at 30°. The return from this beam is therefore attributed to a shallower depth, Z1, by the ADCP software. Because the beam is emitted at a shallow angle (relative to vertical), the Doppler shift of the beam during emission **while underway** is reduced, the return signal is of lower frequency than would be expected if the beam were emitted at 30°, and the ocean velocity measured relative to the ship is biased towards zero. When adding ocean velocity (relative to the ship) to ship velocity (relative to earth) to calculate absolute ocean velocities, a bias therefore remains in the direction of ship motion at depths shallower than the scattering layer. This effect is reversed for side lobe beams emitted at a steeper angle (relative to vertical) leading to a bias in absolute ocean velocities opposite to ship motion at depths below the scattering layer. Although side lobes contain less energy than the main beam at 30°, the presence of a strong scattering layer mean their effects become noticeable and in this case dominant. This effect is not noted in across track velocities because there is much less Doppler shift during beam emission perpendicular to the direction of ship motion.

The result of this 'high backscatter layer' is an 'S' shaped bias in ocean velocity measurements, with a crossing point centred on the high backscatter layer itself. The 'S' can extend to a range of several bins above and below the centre of the high backscatter layer. This bias is present in the ADCP velocities shown in figure 2 (top) from approximately 350 metre depths to the range of the instrument. However, because of the limited range of the ADCP, the full 'S' shape of the bias cannot be discerned. When ship velocity reduces, this bias should also reduce and eventually disappear. Figure 9 shows ship speed measured by the GPS (top), hourly velocity profiles measured by the ADCP (middle) and three-hourly backscatter intensity (bottom) for the period surrounding CTD casts 8 and 9. Although the high scatter layer is present throughout, the velocity bias diminishes during periods of reduced ship speed for CTD operations. This contrasts with figure 10, showing ADCP measurements during the transit from Falmouth to Tenerife. Although an error with the GPS led to a reduced number of available ocean velocity profiles, it is still evident that during periods of steaming, there is no ADCP velocity bias at depth because no strong backscattering layer is present. Further plots (not shown) show that this deep scattering layer is present shortly after leaving Tenerife (day 288). The bias is not as evident in figure 3 (top) during this period because the south westerly heading of the

ship prior to day 292 means some component of the zonal velocity is measured across track which reduces the impact of this along track bias. No method for removing this bias attributable to a deep scattering layer is apparent. Because some of the zooplankton layer remains in situ (at 470 metres) both night and day (i.e. does not migrate diurnally, see figure 3 bottom), the velocity bias is present throughout the whole ADCP dataset and therefore little good data for this depth range are available. The persistence of such signals in single-ping .ENX data would be worth investigating to see if any data could be salvaged at depth where a strong scattering layer occurs.

4.2 OS75-Geostrophy Comparison

Comparison of ADCP data to geostrophic velocities calculated between CTD stations 5-10 in the upper water column are shown in figure 11. Data shown was collected during transit to the MAR and for geostrophic purposes assumes a depth of no motion at 3200 metres. The CTD data used was not calibrated to samples collected on D324 however the CTD was relatively well calibrated at the start of the trip. The effect of erroneous E-W ADCP velocity measurements (discussed above) is small due to predominant analysis of the N-S component of ADCP measurements. Of particular note are the velocity profiles averaged between station pair 7-8 (between 23-41W and covering the widest area). Geostrophic velocity decreases steadily from -1.5 cms^{-1} at the surface to 0 cms^{-1} at 1000m, while the ADCP velocity shows broadly similar structure (except above 50m depths where inertial effects dominate) but offset such that velocity approaches +1.5 cms^{-1} at 600m. Adjustment of geostrophic velocity to match this absolute velocity would lead to anomalously large ocean transports at depth. Velocities between stations 6 and 7 again show broadly similar profiles but are offset. Little agreement is seen between absolute ADCP velocity and geostrophic velocity for station pairs 5-6 and 8-10 (the latter over the MAR).

5. Conclusion

The setup, processing and results from the underway ADCP during cruise D324 have been described. Of particular note are three potential biases observed in the data. The first of these is a series of vertical velocity bands (10-15 cms^{-1} magnitude) observed in both the along track and cross track measurements. A heading error is ruled out as the source of this signal, suggesting the banding observed is real. Comparison with a tidal model suggests velocity bands are not of tidal origin, implying a strong eddy field. The second bias is an along track forward bias caused by bubble interference with the ADCP signal. It is shown that this bubble bias produces two distinct velocity profile types, which can be removed from the measurements by applying filters to the raw, single-ping .ENX files. Algorithms are applied that remove short profiles and shear outliers before averaging to .STA files. Data showing a degraded % good measurement near the surface are then also removed. Application of such algorithms is recommended in the future where appropriate, however care should be taken to choose suitable filter parameters for a particular dataset. The final bias is an S-shaped velocity structure in the along track data that appears due to interaction of the ADCP side lobes with a strong scattering horizon. This bias relies on differences in Doppler shift between the side lobe and main beams during emission and as such is only observed while underway. The absence of the bias during periods when the ship was stationary or when no scattering layer was observed is demonstrated. Diurnal

migration of the strong scattering layer (seen in ADCP backscatter intensity measurements) suggests it is a biological horizon. ADCP data are contaminated by this bias for the duration of D324. Similar velocity biases have been observed elsewhere in the ocean.

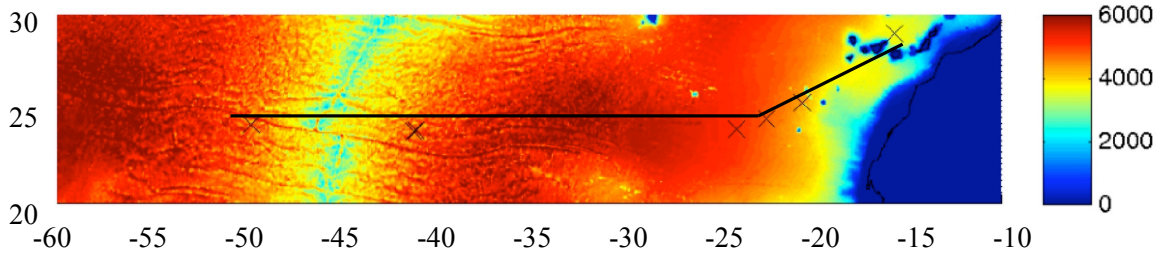

Figure 1, D324 Cruise Track on bathymetric map (longitude vs. latitude, depth in metres).

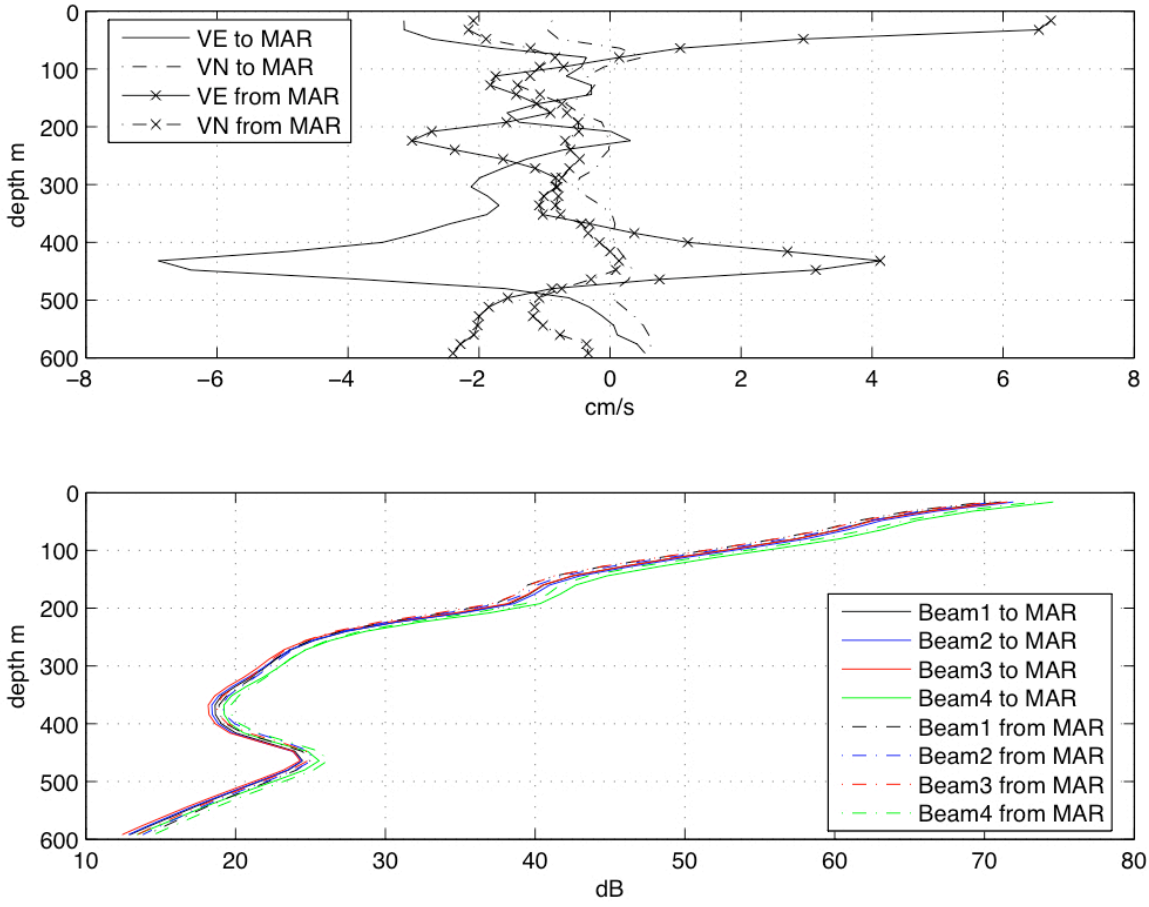

Figure 2. Meridional (VN) and zonal velocity (VE) components (top) and beam intensity (bottom) measured by the ADCP during transit to and from the MAR during D324. Bins are averaged longitudinally between 20 and 50 W.

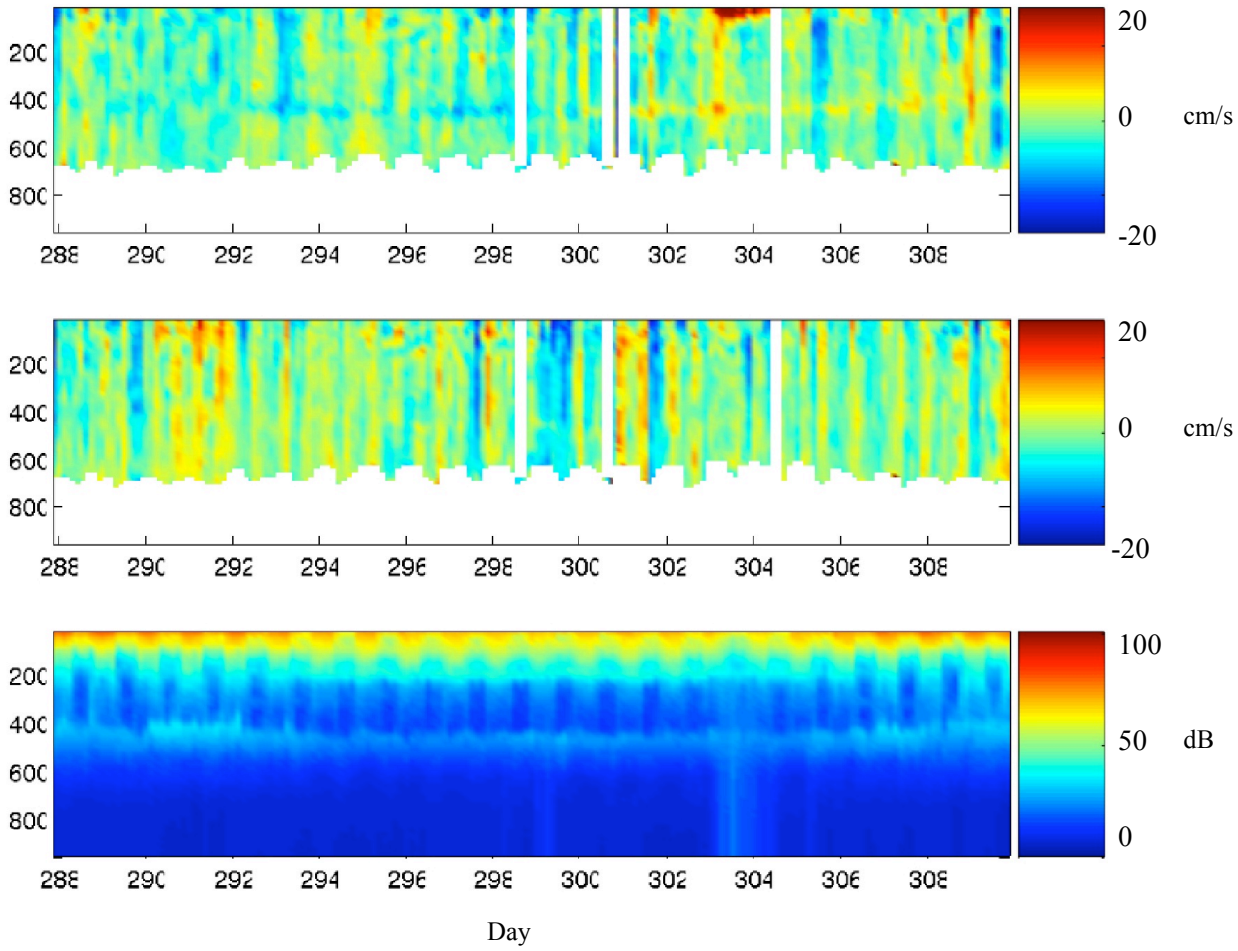

Figure 3. Zonal ocean velocity (top), meridional ocean velocity (middle) and beam 1 intensity (bottom) against depth (m) measured by the ADCP during transit to and from the MAR during D324.

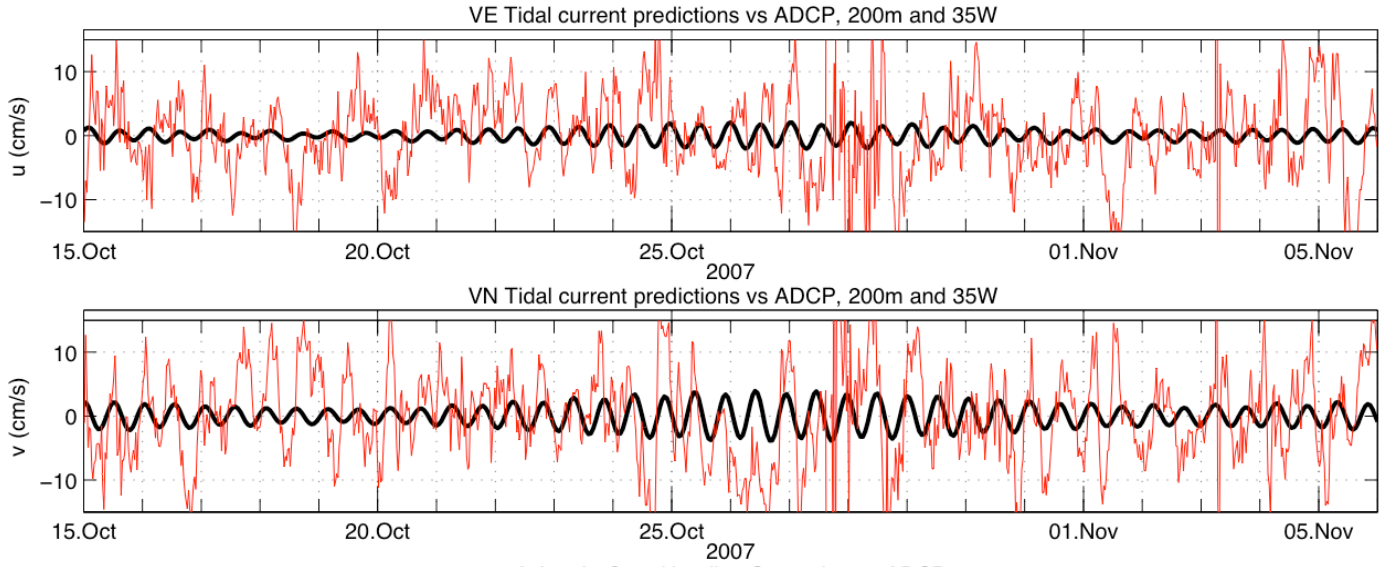

Figure 4. ADCP (red lines) zonal (top) and meridional (bottom) velocities during cruise D324 and tidal velocities (black lines) predicted from a tidal model. Velocities are shown at 200m depth. Tidal velocities are calculated using harmonic constituents at 26N, 35W (note, tidal harmonics are relatively longitudinally invariant at this latitude).

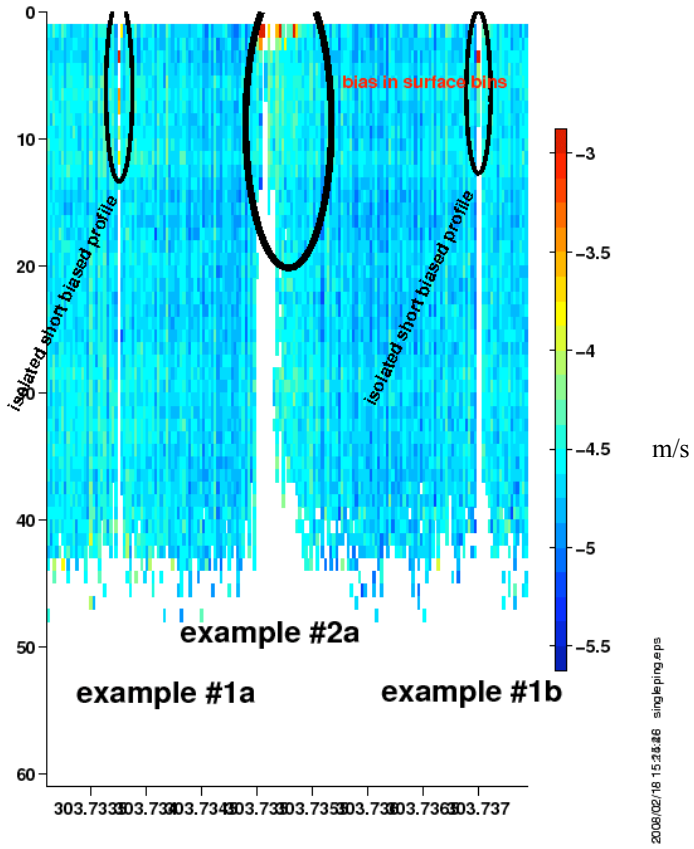

Figure 5. Plot showing single-ping (.ENX) along track velocities versus bin number for part of day 303. Two types of bubble related bias are highlighted. Courtesy of Julia Hummon, University of Hawaii.

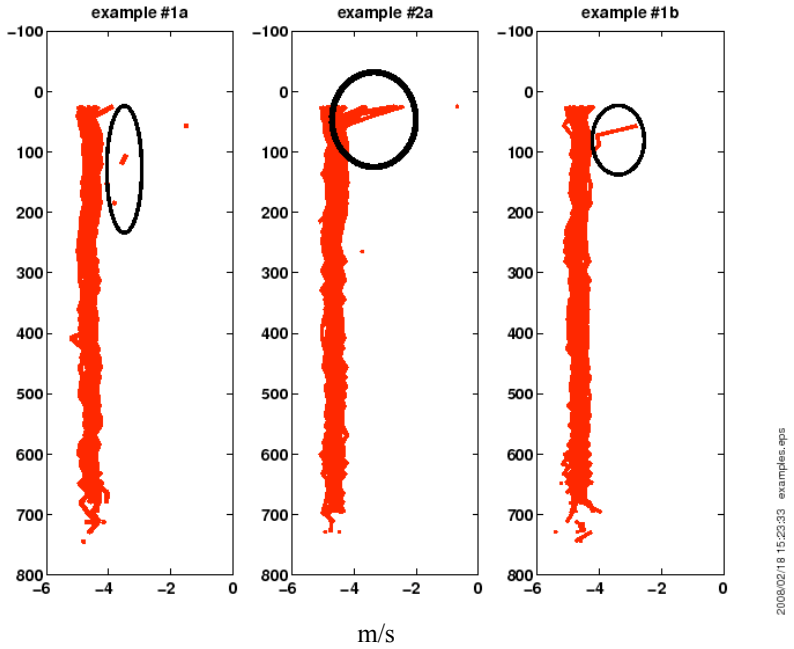

Figure 6. Along track velocity profiles of two types of bubble bias highlighted in figure 4. Courtesy of Julia Hummon, University of Hawaii.

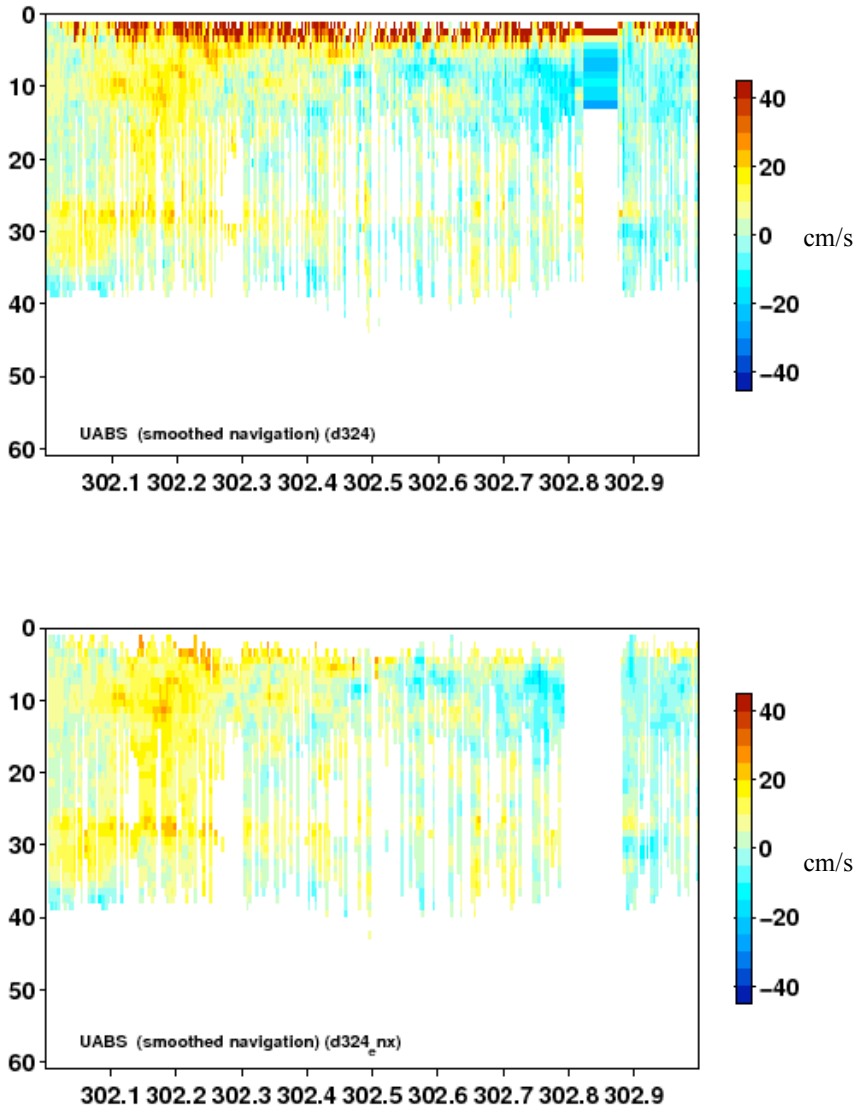

Figure 7. Plots of zonal velocity versus bin number for day 303. Top shows .STA data without .ENX editing routines. Bottom shows .STA data formed using edited .ENX files. Courtesy of Julia Hummon, University of Hawaii.

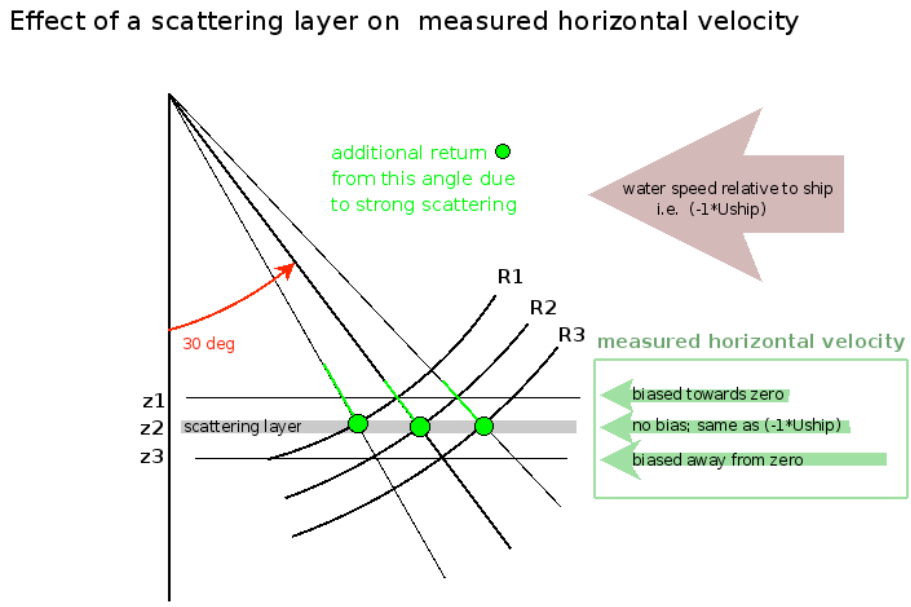

Figure 8. Schematic diagram demonstrating the effects of a strong scattering layer on an ADCP beam and measured velocities (courtesy Julia Hummon, University of Hawaii), see text for explanation.

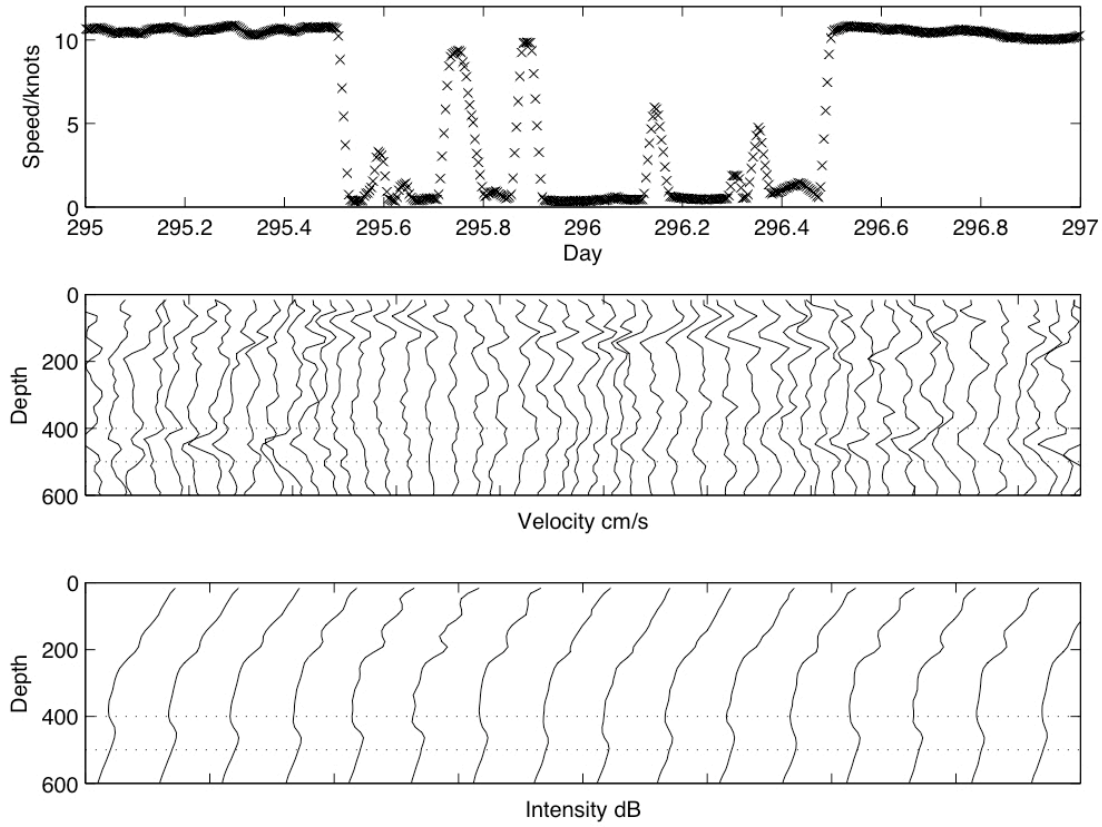

Figure 9. Ship speed (top), hourly velocity profiles (middle), and three hourly ADCP beam 1 intensity profiles (bottom) for from day 295 to 297. Depths of interest are highlighted by stippled lines. One velocity axis tick corresponds to 50 cms^{-1}, one intensity axis tick corresponds to 100 dB.

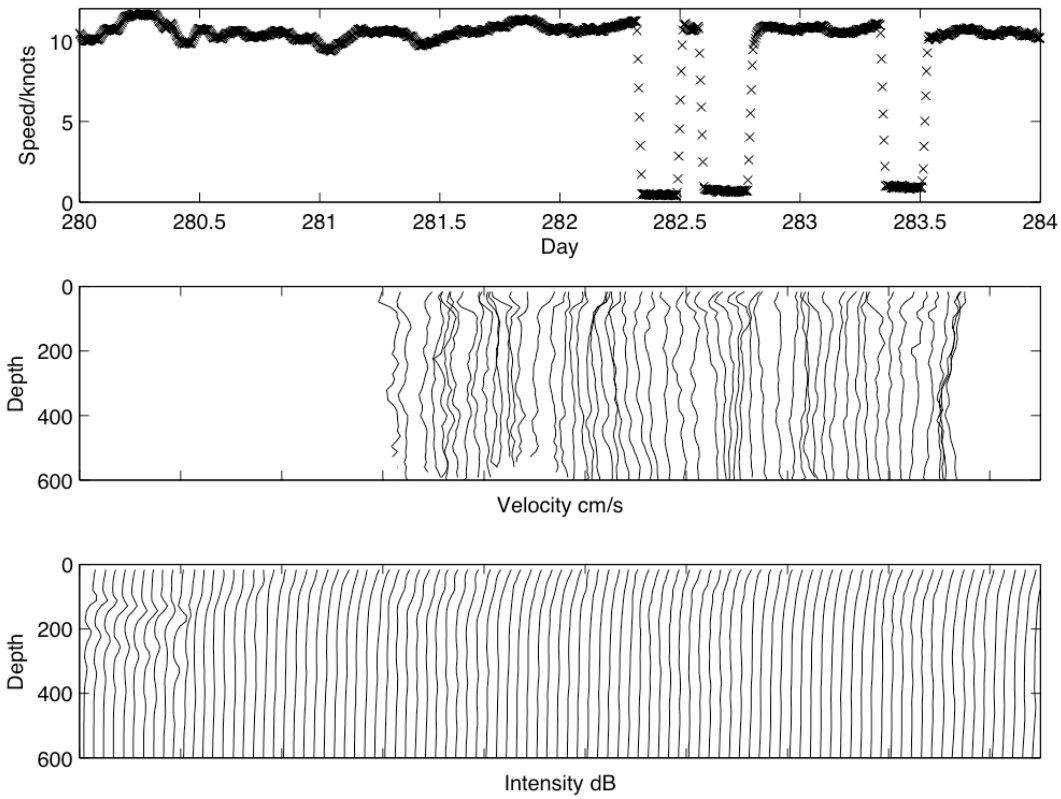

Figure 10. As for figure 8, ADCP beam 1 intensities (bottom) are shown hourly. Velocity data is absent for much of the transit due to a GPS error.

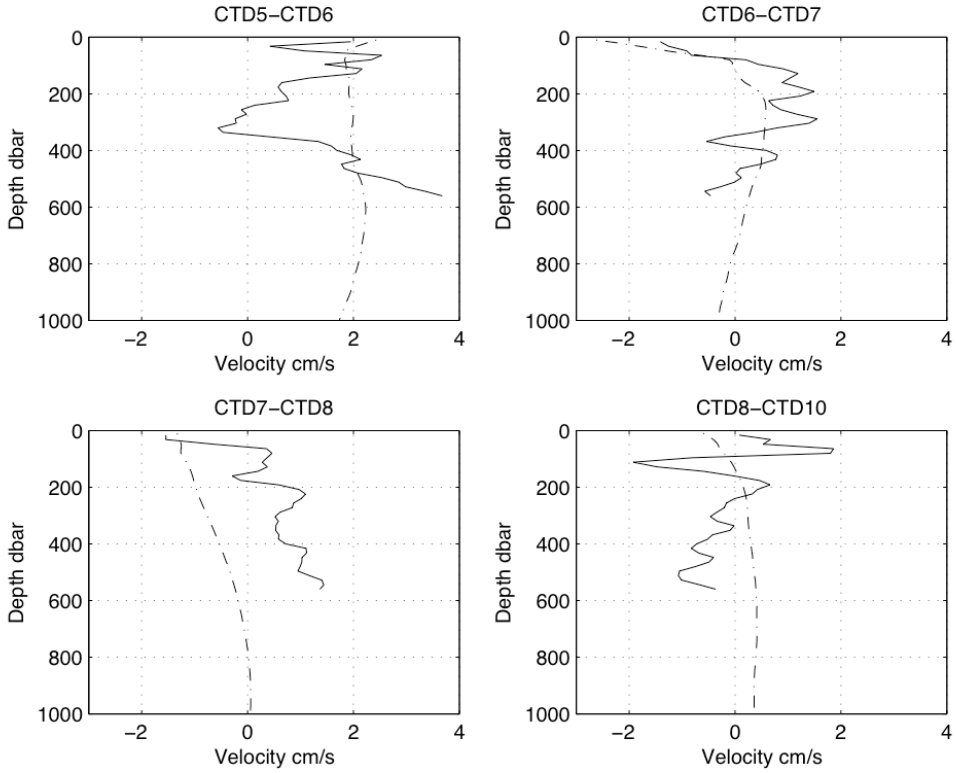

Figure 11. Geostrophic velocities (stippled line) and ADCP velocities (solid lines) averaged between CTD station pairs.